Vacancylike structure of the *DX* center in Te-doped $Al_xGa_{1-x}As$

T. Laine, J. Mäkinen, K. Saarinen, and P. Hautojärvi
Laboratory of Physics, Helsinki University of Technology, 02150 Espoo, Finland

C. Corbel
Institut National des Sciences et Techniques Nucléaires, Centre d'Etudes de Saclay, 91191 Gif-sur-Yvette Cedex, France

M. L. Fille and P. Gibart
Centre de Recherche sur l'Hétéro-Epitaxie et ses Applications, Centre National de la Recherche Scientifique, Sophia Antipolis, 06560 Valbonne, France

(Received 3 October 1995; revised manuscript received 21 December 1995)

The positron-annihilation method was used to investigate the *DX* centers in Te-doped $Al_xGa_{1-x}As$ grown by metal-organic vapor-phase epitaxy. Vacancy defects were found in all layers. The vacancy signal disappears when the *DX* center is ionized either optically or thermally. After the optical ionization the vacancy signal reappears when the temperature increases over 50 K. The optical cross section of 4×10^{-17} cm^2 was determined for the removal of the positron trapping at a vacancy. Because the properties of the vacancy signal correlate exactly with those determined earlier for the *DX*(Te) center, we conclude that the vacancy detected by positrons belongs to the atomic structure of the *DX*(Te) center. This result is in agreement with the vacancy-interstitial model, which predicts that in the case of group-VI(Te) doping the *DX* center is formed by the distortion of the Ga atom towards the interstitial position. The positron results indicate further that the open volume of the vacancy related to the *DX*(Te) center is smaller compared to an isolated monovacancy in GaAs or to the vacancy in the *DX*(Si) center in $Al_xGa_{1-x}As$. This means that the distortion in the vacancy-interstitial configuration is smaller in the *DX*(Te) than in the *DX*(Si) center.

I. INTRODUCTION

Point defects in compound semiconductors have been studied intensively due to their technological importance. The *EL*2 defect[1] in GaAs and the *DX* center[2,3] in $Al_xGa_{1-x}As$ are examples of such defects. *EL*2 is a native midgap donor which compensates the residual acceptor impurities and makes undoped GaAs semi-insulating. The *DX* center limits the free-electron concentration in *n*-type $Al_xGa_{1-x}As$ when $x\geqslant0.22$, and it appears in many other III-V alloys and compounds. The *EL*2 defect and the *DX* center are also well-known examples of the defect metastability in semiconductors.

DX centers are now understood to arise from isolated group-IV and group-VI impurities.[4] Unlike standard donors, *DX* centers are characterized by a large difference between thermal and optical ionization energies. This is taken to indicate that impurity atoms are strongly coupled to the host lattice. The metastability of the *DX* center has been associated with two different configurations[5] of the donor separated by capture and emission barriers. One is the ordinary substitutional donor which gives rise to effective-mass states. The other is characterized by a large (>1 Å) displacement of either the impurity atom or a neighboring Ga atom along a ⟨111⟩ direction. In the distorted geometry, the displaced atom has moved towards the interstitial site. It is threefold coordinated, and the bonding is largely sp^2 like.

The interesting question is how the atomic structure of the *DX* center changes when the group-IV(Si) impurity is replaced by the group-VI(Te) impurity. In the case of Si the impurity is in the group-III(Al, Ga) sublattice and in the case of Te the impurity is in the group-V(As) sublattice. According to the vacancy-interstitial model,[5] in the case of group-IV(Si) doping, the impurity (Si) atom moves and a Ga vacancy is formed. In the case of group-VI(Te) doping, one of the neighboring Ga atoms moves and again a Ga vacancy is formed. Nevertheless, only few experimental results exist on the microscopic structure of the *DX* center in Te-doped AlGaAs.[6]

Positron annihilation spectroscopy is a nondestructive method to study vacancy defects in semiconductors. This technique has earlier been used to investigate the local structure of the *DX* center in Si- and Sn-doped $Al_xGa_{1-x}As$ (Ref. 7) as well as in Te-doped $Al_xGa_{1-x}Sb$.[8] Direct experimental evidence of the vacancylike structure of the *DX* center was found in all cases. The open volume of the *DX* center in $Al_xGa_{1-x}As$ is less than that of Ga or As monovacancies in GaAs. The structural data from the positron annihilation experiments give support to the vacancy-interstitial model,[5] which predicts a displacement of the group-IV donors (Si, Sn) towards the interstitial site and a formation of a Ga vacancy in $Al_xGa_{1-x}As$.

In this paper the positron-annihilation method is used to study the *DX* center in $Al_xGa_{1-x}As$ doped with Te which is a group-VI donor at an As site. The main idea is to compare the positron results in *n*-type $Al_xGa_{1-x}As$ when the group-IV(Si) impurity is replaced by the group-IV(Te) impurity. We report the vacancylike structure of the *DX* center in Te-doped $Al_xGa_{1-x}As$. Our results are in good agreement with the vacancy-interstitial model, which predicts a formation of a Ga vacancy through a displacement of a Ga atom next to a group-VI donor.

 © 1996 The American Physical Society

TABLE I. Characteristics of the Te-doped MOVPE-grown $Al_xGa_{1-x}As$ layers. The Hall carrier concentration n_{Hall} is given at 4 K before and after light illumination with 1.4-eV photons. The Te concentration N_{Te} was estimated to be $\approx 2\times10^{18}$ cm^{-3} for samples (2) and (3). For comparison, one undoped $Al_xGa_{1-x}As$ sample (4) was measured. X is the measured AlAs mole fraction and D is the layer thickness.

Sample	X	D (μm)	N_{Te} (cm^{-3})	n_{Hall} (cm^{-3}) dark	n_{Hall} (cm^{-3}) illum.
1	0.07		7×10^{18}		
2	0.27	2.8	2×10^{18}	5.0×10^{17}	2.0×10^{18}
3	0.27	5	2×10^{18}	5.0×10^{17}	1.7×10^{18}
4	0.25		Undoped		

II. EXPERIMENTAL DETAILS

Te-doped $Al_xGa_{1-x}As$ samples (Table I) were grown by metal-organic vapor-phase epitaxy (MOVPE) on GaAs(100) substrates. The AlAs fractions in the samples are $x=0.07$ (sample 1) and $x=0.27$ (samples 2 and 3). The AlAs fractions were measured by double x-ray diffraction and by electron microprobe analysis, and the error was estimated to be smaller than 0.01. Samples 2 and 3 have a similar structure with a buffer layer followed by a 3-μm Te-doped $Al_{0.27}Ga_{0.73}As$ layer. The buffer layer consists of 1-μm undoped $Al_{0.7}Ga_{0.3}As$ followed by a 1-μm undoped $Al_{0.27}Ga_{0.73}As$ layer. For Te doping, $Te(C_2H_5)_2$ diluted in pure hydrogen was used as a precursor. In sample 1, the Te concentration is 7×10^{18} cm^{-3}. In samples 2 and 3 the Hall carrier concentration at 4 K after illumination is $n_{Hall}=2\times10^{18}$ cm^{-3}. Based on this the Te concentration for these samples is $\geqslant 2\times10^{18}$ cm^{-3}. For comparison we measured an undoped $Al_{0.25}Ga_{0.75}As$ layer (sample 4) grown by molecular-beam epitaxy (MBE).

Electrical measurements have been performed on Te-doped $Al_xGa_{1-x}As$ samples. The free-carrier concentration was determined using both Hall and Shubnikov–de Haas (SdH) effects. To obtain the most accurate measurements at low temperature, Hall bar-shaped samples have been designed through a photolithography process. The electrical contacts had been made with a Au-Ge alloy.

The sample was mounted in a cryostat and the measurement of the free-carrier concentration as a function of the temperature was taken in two steps (rate of ±2 K/mn). First, the temperature was decreased from 300 to 4.2 K and the measurements were taken in the dark. At 4.2 K, the sample was illuminated with a 1.4-eV light-emitting diode to saturate the persistent photoconductivity. At this temperature, the SdH effect was taken to verify the value of the free-carrier concentration measured by the Hall effect. It was found that there was very good agreement between the two values.

Then, the temperature is raised up to 300 K. The advantage of this experimental temperature cycle (see Fig. 1) is the precise determination of the temperature at which the DX centers are in thermal equilibrium with the conduction band. This means that the value of the free-carrier concentration taken in the dark and after illumination is the same. This will be useful for the interpretation of the results obtained with the positron-annihilation experiments.

Positron annihilation in the epitaxial layers was measured using the low-energy positron-beam technique.[9] The 511-keV annihilation spectra were detected and recorded with a high-purity Ge detector and a digitally stabilized multichannel analyzer system. More than 3×10^6 counts were collected to the annihilation peak in each measurement. The sample temperature was controlled between room temperature and 20 K with a closed-cycle He cryocooler and it was measured with a silicon diode temperature sensor. Above room temperature the sample was heated with an electron-beam heater, and its temperature was measured with a type-K thermocouple mounted onto the sample surface. The accuracy of the temperature measurement was estimated to be better than ±2 K. Samples were illuminated with GaAs-infrared diodes the maximum intensity of which is at 940-nm wavelength (1.32 eV). The light intensity measured with a Ge photodetector was 0.1 mW/cm^2, corresponding to the photon flux of 2×10^{14} s^{-1} cm^{-2} at the surface of the sample.

Doppler broadening of the annihilation radiation gives information on the momentum distribution of annihilating electrons. The shape of the 511-keV annihilation line convoluted with the resolution of the Ge detector is described in terms of valence and core annihilation. The valence annihilation parameter (S) is defined as the ratio of annihilation events over the energy range (511 ± 0.95) keV around the centroid of the peak to the total number of events in the annihilation line. It represents the electron-positron pairs

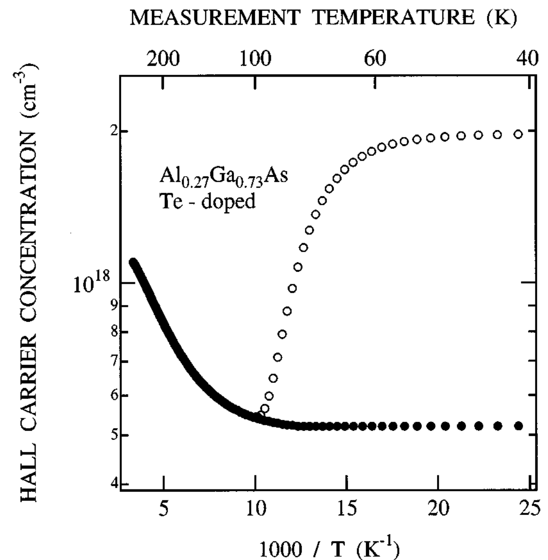

FIG. 1. Temperature dependence of the carrier concentration $n_{Hall}=-1/eR_H$ for Te-doped $Al_{0.27}Ga_{0.73}As$ (sample 2). The carrier concentration was first measured in the dark (●) and then after illumination (○), which was done at 4 K by an infrared light-emitting diode with 1.4-eV photons. The onset for the decay of the persistent photoconductivity is at 50 K and the photoconductivity is fully quenched at 100 K.

with a longitudinal momentum component $p_L/m_0c \leq 3.7 \times 10^{-3}$, which are mainly due to the annihilations with the valence electrons (m_0 is the electron mass and c is the speed of light). The core annihilation parameter (W) is defined as the ratio of the annihilation events in the tail of the peak, 2.9 keV$\leq |E-511$ keV$| \leq 7.3$ keV (or $11 \times 10^{-3} \leq p_L/m_0c \leq 28 \times 10^{-3}$). As defined here, it corresponds to annihilations with the core electrons. The defect-specific parameter $R=(S-S_B)/(W_B-W)$ can be defined as the ratio of the changes in S and W parameters compared to their values in defect-free crystal (S_B, W_B). The R parameter can be used to distinguish different defects.[10,11]

The coincidence technique can be used to reduce the background level in the high-energy side of the 511-keV peak.[12] In order to study the high momentum tails of the Doppler spectra, we used a NaI detector (1.5 in.×2 in.) in coincidence with a high-purity Ge-detector (2.5 in.×2 in.). In this setup we obtained the peak-to-background ratio of 1.7×10^4 on the high-energy side of the 511-keV peak. The coincident count rate in the annihilation peak was 80/s and typically 2×10^7 counts were collected in every spectrum. All the coincidence measurements were done at room temperature.

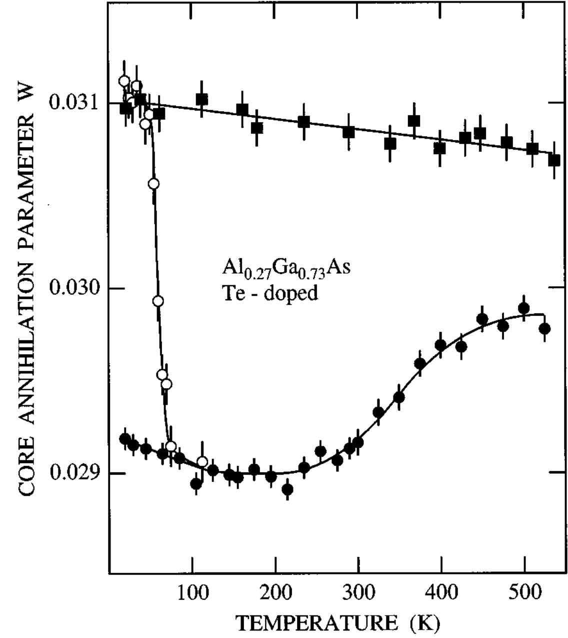

FIG. 2. The core annihilation parameter W as a function of temperature in undoped $Al_{0.25}Ga_{0.75}As$ (sample 4) (■) and in Te-doped $Al_{0.27}Ga_{0.73}As$ (sample 3) (●) between 20 and 500 K. The vacancy signal disappears when the sample is illuminated (○) at 20 K with 1.32-eV photons. The vacancy signal is fully recovered when the temperature is increased from 50 to 70 K after illumination at 20 K. A part of the vacancy signal disappears when the temperature is increased from 300 to 500 K.

III. RESULTS

A. Photo-Hall measurements

The Hall carrier concentration $n_{\text{Hall}}=-1/eR_H$ for Te-doped $Al_{0.27}Ga_{0.73}As$ (sample 2) is plotted against the reciprocal temperature $1/T$ between 40 K and room temperature in Fig. 1. In this sample, the buffer layer was used to prevent the formation of an n-type channel at the interface between the n-type layer and the semi-insulating GaAs substrate, which could lead to a complicated multilayer conduction.

The black dots in Fig. 1 correspond to the measurements during cooling of the sample in the dark. In the temperature range from 300 K to approximately 170 K, n_{Hall} in the dark is an exponential function of temperature, and the apparent activation energy determined from the Arrhenius plot is 15 meV. Below 100 K the free-electron concentration is nearly independent of temperature, and cooling down to 4 K showed no evidence of the freeze-out of electrons. Such temperature behavior has been observed in $Al_xGa_{1-x}As$ when the shallow donor level and the DX level coexist in the band gap.[13] In the high-temperature region above 100 K the DX state participates in the carrier distribution between the conduction band and the defect states. The abrupt change in the slope marks the temperature range below which the DX level does not take part in the electron exchange with the conduction band. This is due to the exceedingly small electron capture rate at the DX center in the low-temperature limit.[2,3]

To illustrate the persistent photoconductivity, the Hall carrier concentration was measured after illuminating the sample with IR light around 1.4 eV at 4 K (Fig. 1). Compared to $n_{\text{Hall}}=5 \times 10^{17}$ cm^{-3} measured after cooling the sample in the dark, a pronounced increase of the Hall carrier concentration to 2×10^{18} cm^{-3} is observed after illumination. Under photoexcitation, electrons are transferred to the Γ conduction band from which they do not repopulate the DX state due to a thermal barrier. Under the persistent photoconductivity conditions the electron concentration is independent of temperature. This is due to the rather high Te doping and the small thermal depth of the shallow donor levels related to the Γ conduction band, resulting in metallic behavior. In this case, all Te atoms are ionized and the Hall carrier concentration obtained at 4 K after photoionization is roughly to the concentration of Te atoms. The onset for the decay of persistent photoconductivity is at 50 K, and by 100 K the electron concentration n_{Hall} coincides with that measured in the dark.

B. Positron trapping at vacancy defects

Positron annihilation was measured in Te-doped $Al_{0.27}Ga_{0.73}As$ and in undoped $Al_{0.25}Ga_{0.75}As$ between 20 and 600 K. The experiment was done with a constant incident positron energy of 15 keV. This corresponds to the mean positron stopping depth of ~0.5 μm in $Al_xGa_{1-x}As$. With this incident energy the contributions from the annihilation events at the surface and in the substrate were negligible.

The core annihilation parameter W for Te-doped $Al_{0.27}Ga_{0.73}As$ (sample 3) and for undoped $Al_{0.25}Ga_{0.75}As$ (sample 4) is plotted against temperature in Fig. 2. The W parameter in undoped $Al_xGa_{1-x}As$ layers gives a reference for free-positron annihilation.[14] The value of the W parameter decreases in undoped $Al_xGa_{1-x}As$ layers when the AlAs mole fraction increases.[7] This is due to the different electron shell structures, which indicates that the core annihilation probability is bigger for GaAs than for AlAs.[15] In the undoped ($x=0.25$) and Te-doped ($x=0.27$) layers the alloy

compositions are, however, so close that the same value of W for free positrons in both layers is anticipated.

The W parameter is systematically lower in the Te-doped sample than in the undoped sample between 20 and 300 K. This means that the annihilation probability with the core electrons is smaller in Te-doped $Al_{0.27}Ga_{0.73}As$, which is typical for samples containing vacancy defects. The R parameter characterizing the vacancy defect is $R=0.9\pm0.1$ at 20–300 K. Between 300 and 500 K the core annihilation parameter increases towards a level which still is well below that in undoped $Al_xGa_{1-x}As$. At the same time, the R parameter also increases, indicating that the defect trapping positrons between 300–600 K are different from the ones between 20–300 K. However, the value of the R parameter cannot be accurately determined because the S and W parameters are too close to their bulk values. These changes of the W and R parameters above room temperature are fully reversible, which means that it is not due to annealing of defects.

Sample 2 was also measured as a function of temperature between 20 and 600 K. The annihilation parameters W and R are identical with those of sample 3 in the temperature range from 20 to 300 K indicating positron trapping at similar vacancies in both layers that have the same alloy composition and Te concentration. However, above room temperature the core annihilation parameter in sample 2 does not increase, but decreases slightly between 300 and 400 K. Similarly as in sample 3, the R parameter increases towards 1.4 ± 0.1 in this temperature range, indicating that a different defect starts to act as a positron trap at $T>300$ K. The R parameter in this sample is much more accurate than in sample 3 because the S and W parameters between 400–600 K remain more distant from the bulk levels (S_B, W_B).

To demonstrate the influence of the alloy composition, the Te-doped $Al_{0.07}Ga_{0.93}As$ layer (sample 1) was also studied. The core annihilation parameter in this sample is below that obtained in p-type GaAs and those estimated for defect-free $Al_{0.07}Ga_{0.93}As$ (Ref. 7) indicating the presence of vacancy defects also in this layer.

C. Removal of the vacancy signal by illumination

In order to see whether the vacancies in Te-doped samples exhibit the metastability associated with the DX center, the annihilation spectra were measured after illumination at 20 K. The core annihilation parameter W after illumination is plotted for Te-doped $Al_{0.27}Ga_{0.73}As$ (sample 3) in Fig. 2. Illumination with IR light increases the value of the W parameter. This phenomenon is persistent at 20 K. After illumination, the W parameter is equal to that measured in undoped $Al_{0.25}Ga_{0.75}As$, indicating that the vacancy signal has completely disappeared.

After illumination the vacancy signal reappears by raising the sample temperature. This is seen as the abrupt decrease of the W parameter from the level of the undoped layer. The onset for the recovery is around 50 K and the recovery is completed at 70 K. The core annihilation parameter was also measured as a function of the isochronal annealing temperature for the same Te-doped $Al_{0.27}Ga_{0.73}As$ sample. As shown in Fig. 3, measurements at 20 K and at the annealing temperature yield similar stages of the recovery of the vacancy signal after illumination at 20 K. In sample 2, the removal of the vacancy signal by IR light and its recovery is very similar to those in sample 3.

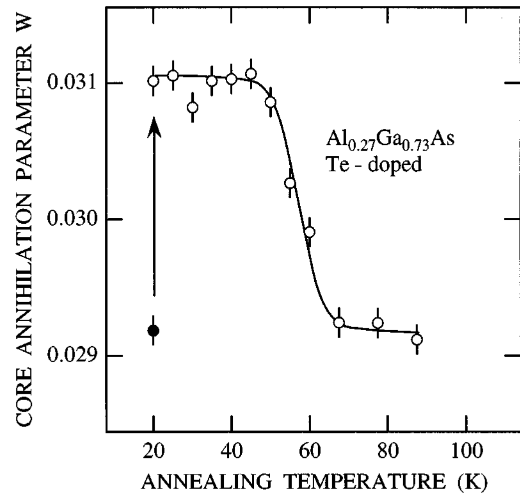

FIG. 3. The core annihilation parameter W as a function of the isochronal annealing temperature for Te-doped $Al_{0.27}Ga_{0.73}As$ (sample 3) (○) after illumination at 20 K. The vacancy signal disappears when the sample is illuminated with 1.32-eV photons and it recovers when the annealing temperature rises from 50 to 70 K.

In the case of Te-doped $Al_{0.07}Ga_{0.93}As$ (sample 1), the illumination effect is not seen at 20 K. The core annihilation parameter is also unchanged in undoped $Al_{0.25}Ga_{0.75}As$ (sample 4) before and after illumination at 20 K.

It can be summarized that the vacancy defects can be persistently removed by illumination in the samples which are Te doped and in which the AlAs mole fraction is ≈ 0.27.

D. Determination of the optical cross section for the photoquenching of the vacancy

The removal of the vacancy signal was also measured as a function of the time for illumination and keeping the photon flux constant $\Phi=2\times10^{14}\ \mathrm{s}^{-1}\ \mathrm{cm}^{-2}$. In practice, the removal of the vacancy signal is then measured as a function of the illumination fluence (Φt). When the total photon fluence increases, the core annihilation parameter W increases smoothly in Fig. 4, and by the photon fluence of 1×10^{17} cm^{-2} it reaches the level of free-positron annihilation.

We use the kinetic positron trapping model[16] to estimate the optical cross section describing the removal of the vacancy signal. When positrons are trapped at vacancies, the positron trapping rate κ_v is proportional to the ratio of the core annihilation parameters as

$$\kappa_v=\kappa_0\,\frac{W_B-W}{W-W_D}. \quad (1)$$

In Eq. (1) the prefactor κ_0 is equal to the annihilation rate λ_B of free positrons, if there is no positron annihilation at the Rydberg state of negative ion-type centers. W_B and W_D denote the core annihilation parameters for free-positron annihilation and for the vacancy. As the core annihilation parameter after illumination is equal to W_B, the photoquenchable vacancy is the dominant vacancy-type positron trap at

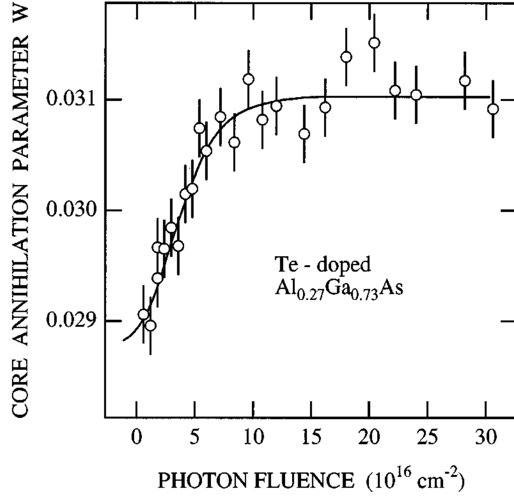

FIG. 4. The core annihilation parameter (○) as a function of photon fluence in Te-doped $Al_{0.27}Ga_{0.73}As$ (sample 3). The photon energy was 1.32 eV. The change of core annihilation parameter from the vacancy level to the free-positron annihilation level is complete when the photon fluence is 1×10^{17} cm^{-2}.

20 K. The core annihilation parameter after illumination at 20 K yields W_B=0.0311(1). Assuming that all positrons are trapped below 200 K (see Sec. IV), the core annihilation parameter at the photoquenchable vacancy is W_v=0.0291(1).

Figure 5 shows κ_v/κ_0 as a function of the photon fluence for Te-doped $Al_{0.27}Ga_{0.73}As$ (sample 3) and for Si-doped $Al_{0.29}Ga_{0.71}As$ from Ref. 14. The fluence dependence of the trapping rate is due to κ_v, since κ_0 is a constant as the measurement was done at a constant temperature at 20 K. The positron trapping rate κ_v decreases exponentially by almost two orders of magnitude. In the Te-doped sample and in the Si-doped sample a different photon fluence is needed in order to get the same effect.

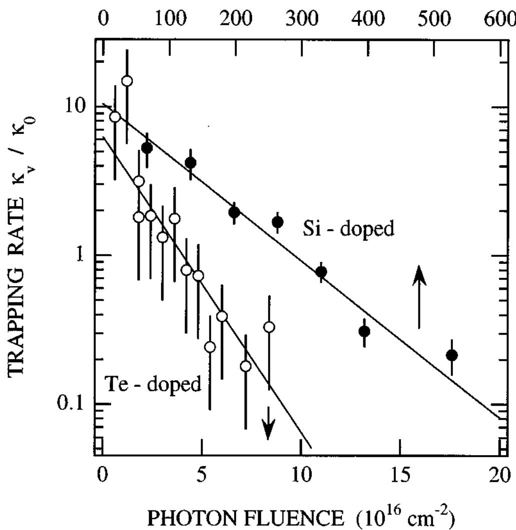

FIG. 5. The positron trapping rate κ (○) as a function of photon fluence in Te-doped $Al_{0.27}Ga_{0.73}As$ (sample 3) and in Si-doped $Al_{0.29}Ga_{0.71}As$ (Ref. 14). The fitted lines correspond to the fits of Eq. (2) with the optical cross section as a free parameter. A photon energy of 1.32 eV was used in the illumination.

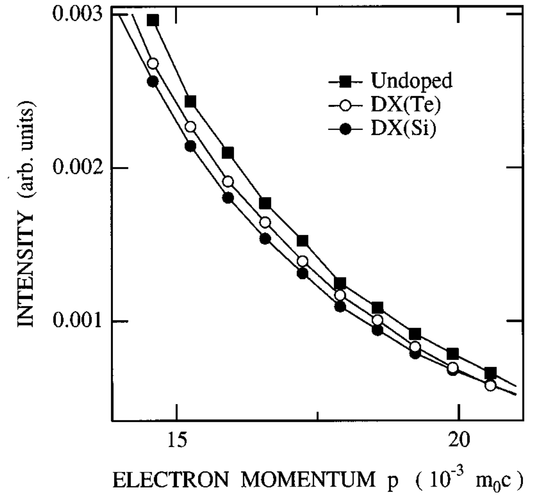

FIG. 6. The intensity of the core annihilation parameter W in undoped $Al_{0.25}Ga_{0.75}As$ (■), in Te-doped $Al_{0.27}Ga_{0.73}As$ (○), and in Si-doped $Al_{0.29}Ga_{0.71}As$ (●). The relative core annihilation parameters at $(15-20)\times10^{-3}m_0c$ are $W_{DX(\mathrm{Si})}/W_B=0.87$ for Si-doped $Al_{0.29}Ga_{0.71}As$ and $W_{DX(\mathrm{Te})}/W_B=0.92$ for Te-doped $Al_{0.27}Ga_{0.73}As$.

The decay of the trapping rate can be fitted by a single exponential function,

$$\kappa=\kappa_0 \exp(-\sigma\phi t), \tag{2}$$

where κ_0 is the trapping rate at the time $t=0$ and $(\sigma\phi)^{-1}$ is the time constant for the decay. The vacancy concentration is given by $C_v=\kappa_v/\mu$, where μ is the positron trapping coefficient. The trapping coefficient μ is constant if the temperature does not change.[17] The time constant $(\sigma\phi)^{-1}$ therefore gives the optical cross section of $\sigma\approx(4\pm2)\times10^{-17}$ cm^2 for Te-doped $Al_{0.27}Ga_{0.73}As$ and $\sigma\approx1\times10^{-18}$ cm^2 for Si-doped $Al_{0.29}Ga_{0.71}As$.[14] These values will be compared with the optical ionization cross sections for the DX(Te) center and for the DX(Si) center in Sec. IV.

E. Core electron momentum distribution

Using the two-detector coincidence technique, the core electron momentum distributions can be measured in the energy window of 3.6 keV$\leqslant|E-511$ keV$|\leqslant$5.4 keV.[12] The longitudinal momentum values of the annihilation pairs are then in the range of $p_L/m_0c=(14-21)\times10^{-3}$. The core electron momentum spectrum was measured for Te-doped $Al_{0.27}Ga_{0.73}As$ (sample 3) and for undoped $Al_{0.25}Ga_{0.75}As$ (sample 4) at room temperature. For comparison, the core electron momentum spectrum was also measured for Si-doped $Al_{0.29}Ga_{0.71}As$, where we have recently detected a vacancy defect related to the DX center.[7] The AlAs mole fractions ($0.25\leqslant x\leqslant0.29$) are so close in these three samples that the core electron momentum distributions can be quantitatively compared without any scaling due to the differences in x.

High-momentum parts of the Doppler curves after area normalization are plotted in Fig. 6. In all three cases the shape of the momentum distribution is same and only the relative magnitudes change. The magnitude of core electron

annihilations is the biggest in undoped $Al_{0.25}Ga_{0.75}As$ and the smallest in Si-doped $Al_{0.29}Ga_{0.71}As$. The Te-doped $Al_{0.27}Ga_{0.73}As$ lies between these two curves. The same observation comes from the W parameter, calculated at $(15-20)\times10^{-3}m_0c$. We get the ratio $W_{DX(\mathrm{Si})}/W_B=0.87$ for Si-doped $Al_{0.29}Ga_{0.71}As$ and $W_{DX(\mathrm{Te})}/W_B=0.92$ for Te-doped $Al_{0.27}Ga_{0.73}As$, where we have used the data obtained in undoped $Al_{0.25}Ga_{0.75}As$ for W_B.

IV. DISCUSSION

A. Identification of the vacancy defects

1. The photoquenchable vacancy

In this section we identify the photoquenchable vacancy in Te-doped $Al_{0.27}Ga_{0.73}As$ as the DX center. This is based on the persistent photoconductivity which is seen in this sample, the comparison of the optical cross sections with those measured for the DX(Te) center, and the phenomenological comparison of present results with those measured earlier for the DX(Si) center in Al_xGa_{1-x} As.[7,14]

Positron annihilation gives direct evidence of the existence of vacancies in n-type Te-doped $Al_{0.27}Ga_{0.73}As$. The photoquenchable vacancy signal is not observed in undoped $Al_{0.25}Ga_{0.75}As$ (sample 4) or in Te-doped $Al_{0.07}Ga_{0.93}As$ (sample 1), so it is correlated with Te-type doping and Al alloying ($x\approx0.27$). Recently the same kind of correlation with Si doping and Al alloying has been observed in Si-doped $Al_xGa_{1-x}As$ when $x\geqslant0.18$.[7]

In Hall data the persistent photoconductivity is seen in Te-doped $Al_{0.27}Ga_{0.73}As$. Illumination at low temperatures converts the deep electron states into shallow donor levels. Thermal equilibrium cannot be reached because of the thermal capture barrier which separates the deep DX level and the shallow donor level. In the positron-annihilation data, positron trapping at the vacancy can be photoquenched at 20 K and the change is persistent below 50 K. The increase of the carrier concentration and the disappearance of the vacancy signal are thus correlated after the illumination of Te-doped $Al_{0.27}Ga_{0.73}As$.

The optical cross section of $\sigma\approx4\times10^{-17}$ cm^2 can be determined for the removal of the positron trapping at a vacancy in Te-doped $Al_{0.27}Ga_{0.73}As$. This value can be compared to the optical ionization cross section for the DX(Te) center in $Al_xGa_{1-x}As$.[3] Lang *et al.* have found that the optical ionization shows a threshold around 600 meV below which no optical ionization is seen. It achieves the maximum value around 1.1 eV above which the cross section saturates. With the photon energy of 1.32 eV, Lang *et al.* measured the optical ionization cross section of $\sigma_0=4\times10^{-17}$ cm^2 for the Te-doped $Al_xGa_{1-x}As$ independently of the variation of alloy composition. Our results $\sigma\approx4\times10^{-17}$ cm^2 are the same as this value. Recently we have also measured the optical ionization cross section of $\sigma\approx1\times10^{-18}$ cm^2 with the same photon energy for Si-doped $Al_{0.29}Ga_{0.71}As$.[7] The result is markedly different from the DX(Te) center, but it is the same value ($\sigma_0=1\times10^{-18}$ cm^2) as measured for the DX(Si) center using the photocapacitance techniques.[18,19]

In Hall data the persistent photoconductivity disappears at $T\geqslant100$ K in Te-doped $Al_{0.27}Ga_{0.73}As$ (Fig. 1). At this temperature free electrons have enough thermal energy to exceed the thermal capture barrier E_b which separates the shallow donor level and the deep DX level. As a result, shallow donor levels convert back into the deep electron states. Positron trapping at the vacancy recovers when temperature is 70 K. The removal of the persistent photoconductivity and the recovery of the vacancy signal thus take place at the same temperature range between 50 and 100 K.

It had been found earlier that the barrier height E_b depends on the alloy composition[4] and the donor species.[3] The electron capture energies E_b of the DX centers related to different donor species (Si, Sn, Te) can be put in the following order: $E_b(\mathrm{Sn})\leqslant E_b(\mathrm{Te})\leqslant E_b(\mathrm{Si})$.[4] It has been found that in Si-doped $Al_{0.29}Ga_{0.71}As$ the quenching of the vacancy signal takes place in the range 70–90 K and in Sn-doped $Al_{0.48}Ga_{0.52}As$ the disappearance of vacancies is only seen under illumination $T>12$ K.[7] The observed recovering temperature 50–70 K of the vacancy signal in Te-doped $Al_{0.27}Ga_{0.73}As$ correlates thus with the barrier height E_b of the DX center and with the previous positron-annihilation experiments.

In the temperature range from 300 to 600 K the core annihilation parameter W increases in Te-doped $Al_{0.27}Ga_{0.73}As$ (sample 3) towards the value determined in undoped $Al_{0.25}Ga_{0.75}As$ (sample 4). Simultaneously, the R parameter increases from the level of $R=0.9\pm0.1$ to $R=1.4$ ±0.1 in sample 2. This behavior indicates that the photoquenchable vacancy with $R=0.9$ gradually ceases to act as a positron trap in the range 300–600 K and another vacancy with the larger R parameter is detected instead. The disappearance of the photoquenchable vacancy correlates well with the thermal ionization of the DX center, which takes place above 200 K in the Hall data of Fig. 1. Recently the thermal ionization of the DX(Si) center has been observed at the same temperature rate also in Si-doped $Al_{0.29}Ga_{0.71}As$.[7] Notice that the W parameter in the range 300–500 K in sample 3 is larger than that in sample 2 due to a smaller concentration of the other vacancy defect, which becomes visible when the DX(Te) centers are ionized thermally.

To summarize, a vacancy is detected by positrons in Te-doped $Al_xGa_{1-x}As$ ($x\approx0.27$), but not in undoped $Al_xGa_{1-x}As$. The vacancy disappears when the DX center is ionized either optically or thermally. The barrier height for the electron capture at the DX center correlates with the recovery temperature of the vacancy signal after illumination. The optical ionization cross section of the DX center is the same as that determined for the removal of the vacancy under illumination. Thus we identify the vacancy to be a part of the DX center.

2. Other positron traps detected in Te-doped $Al_xGa_{1-x}As$

In addition to the DX centers discussed above, other vacancy defects are also observed in all Te-doped $Al_xGa_{1-x}As$ layers. In Te-doped $Al_{0.07}Ga_{0.93}As$ (sample 1), the W parameter is below the level measured in undoped $Al_xGa_{1-x}As$ and p-type GaAs, indicating the presence of vacancy defects. The vacancies are insensitive to light. In Te-doped $Al_{0.27}Ga_{0.73}As$ (sample 2), the W parameter slightly decreases when the temperature rises from 300 to 400 K. In Te-doped $Al_{0.27}Ga_{0.73}As$ (sample 3), the W parameter increases but stays below the level of the undoped $Al_{0.25}Ga_{0.75}As$ (sample 4) at 500 K.

For the vacancy in sample 2 we get $R=1.4\pm0.1$ from the data between 500 and 600 K. This value is different from the value $R=0.9\pm0.1$ of the photoquenchable vacancy. The value $R=1.4$ is typical for residual vacancies, which have a size of a monovacancy.[20] Because the residual vacancies have not been observed in MBE-grown $Al_xGa_{1-x}As$, their presence is probably related to the MOVPE growth of the layer. Nevertheless, the measured Hall data are equal both in samples 2 and 3 at the temperature range from 20 to 300 K.

However, similar kinds of native vacancies have been previously seen in GaAs in which the Si concentration is $[Si]=4\times10^{18}$ cm^{-3}.[14] The vacancy concentration can be estimated if typical core annihilation parameters for monovacancies ($W_v/W_B=0.84$–0.91) in GaAs (Refs. 21 and 22) and for the positron trapping coefficient $\mu=2\times10^{15}$ s^{-1} (Refs. 17, 23–25) at 300 K are assumed. As a result, the vacancy concentration is 10^{16}–10^{17} cm^{-3} for Te-doped $Al_{0.07}Ga_{0.93}As$ and $Al_{0.27}Ga_{0.73}As$. This concentration is more than an order of magnitude less than the concentration of the *DX* centers in the Te-doped $Al_{0.27}Ga_{0.73}As$ layers.

B. Local structure of the *DX* center

In this section we discuss the local structure of the *DX* center in Te-doped $Al_{0.27}Ga_{0.73}As$. The open volume of the vacancy in Te-doped $Al_{0.27}Ga_{0.73}As$ is compared to an isolated monovacancy and to the *DX*(Si) center in Si-doped $Al_{0.29}Ga_{0.71}As$. Finally, the local structure of the vacancy-interstitial model is discussed in the case of group-VI(S, Se, Te) impurities.

The concentration of *DX* centers in the Te-doped layer $x=0.27$ is at the order of 1×10^{18} cm^{-3}. The positron trapping rate κ at the vacancy in the *DX* center can be estimated using the typical trapping coefficient $\mu\approx2\times10^{15}$ s^{-1} at 300 K for vacancies in semiconductors.[17] The estimated value $\kappa=43\times10^{9}$ s$^{-1}\approx10\lambda_b$ is nearly sufficient to trap all positrons because the trapping fraction is then $\kappa/(\kappa+\lambda_b)\geq0.9$. The core annihilation parameter, measured in the dark, is also almost independent of the temperature between 20 and 300 K. We conclude that the positron trapping at the *DX* center is in saturation in the whole temperature range 20–300 K. Under this condition the W parameter value of this level in the range 20–300 K is characteristic of positrons trapped at the *DX*(Te) center: $W=W_{DX(\mathrm{Te})}$.

The core annihilation parameter $W_{DX(\mathrm{Te})}/W_B=0.92$ of the *DX*(Te) center can be compared with other vacancy defects in GaAs. The coincidence experiments of Doppler broadening give a value of $W_v/W_B=0.73$ for a Ga vacancy and $W_v/W_B=0.72$–0.51 for As vacancies in GaAs.[26] According to these results, the open volume of the *DX*(Te) center is smaller compared to that in the isolated monovacancies in GaAs.

We have also measured the characteristic value $W_{DX(\mathrm{Si})}/W_B=0.87$ for positrons trapped at the *DX* center in Si-doped $Al_{0.29}Ga_{0.71}As$. This value shows that the core annihilation spectrum is more intense in *DX*(Te) than in *DX*(Si), a fact which is well seen in Fig. 6, too. A similar change can be seen also in the valence annihilation parameter S which is $S_{DX(\mathrm{Te})}/S_B=1.002(1)$ for Te-doped $Al_{0.27}Ga_{0.73}As$ and $S_{DX(\mathrm{Si})}/S_B=1.004(1)$ for Si-doped $Al_{0.29}Ga_{0.71}As$ and $S_{DX(\mathrm{Sn})}/S_B=1.004(1)$ for Sn-doped $Al_{0.48}Ga_{0.52}As$.[7]

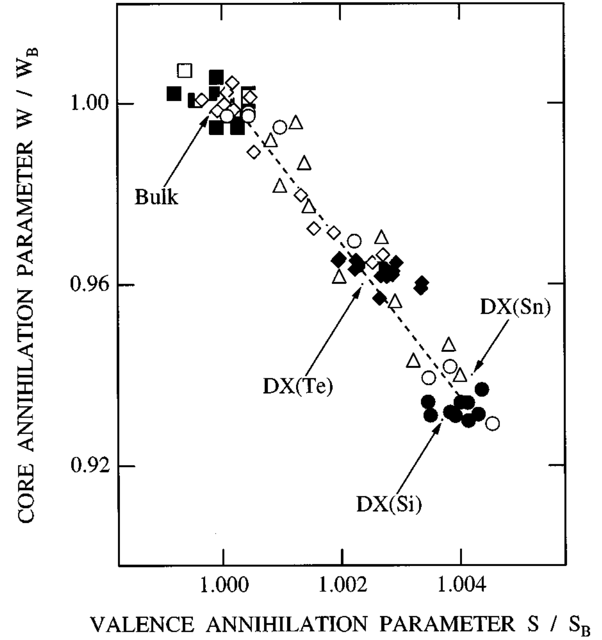

FIG. 7. The core annihilation parameter W as a function of the valence annihilation parameter S for undoped AlGaAs (■), (□), for Te-doped $Al_{0.27}Ga_{0.73}As$ (♦), (◇) and for Si-doped $Al_{0.29}Ga_{0.71}As$ (●), (○). The data are taken from the measurements which have been done in darkness (filled symbols) or after light illumination (open symbols) as a function of temperature in the range 20–200 K. The data for Sn-doped $Al_{0.48}Ga_{0.52}As$ (△) are taken from the measurements above room temperature where the *DX*(Sn) center ionizes thermally (Ref. 7).

In Fig. 7 we have plotted the S and W parameter values measured in the Te-doped $Al_xGa_{1-x}As$, Si-doped $Al_xGa_{1-x}As$, and Sn-doped $Al_xGa_{1-x}As$ layers, where positrons annihilate either as free in the lattice or trapped at *DX*(Te), *DX*(Si), or *DX*(Sn) centers. All the points fall onto the same line showing that the slope $R=\Delta S/\Delta W=0.9\pm0.1$ is the same for *DX*(Te), *DX*(Si), and *DX*(Sn). It has been shown[12,26] that the core annihilation spectrum at $(10$–$30)\times10^{-3}m_0c$ mainly reflects the electron momentum distribution of the outermost core electrons, which are $3d$ for Ga and As, $2p$ for Si, and $4d$ for Sn and Te. If the Si dopant is replaced by the Sn dopant, the number of d electrons increases, which might lead to a more intense core annihilation spectrum and a larger W parameter. However, this does not happen but we get the same valence $S_{DX(\mathrm{Sn})}/S_B=1.004(1)$ and core $W_{DX(\mathrm{Sn})}/W_B=0.940(3)$ annihilation parameters for Sn-doped $Al_{0.48}Ga_{0.52}As$ (Ref. 7) as for Si-doped $Al_{0.29}Ga_{0.71}As$ (Ref. 7) in Fig. 7.

Furthermore, the core annihilation momentum spectra in Fig. 6 show that the shapes of the momentum distributions are similar in *DX*(Si) and *DX*(Te) centers. The $4d$ electrons of Te are less localized than the $3d$ electrons of Ga and As and the $2p$ electrons of Si, which would lead to a narrower shape of the core electron momentum distribution at *DX*(Te).[12,26] However, no such effects are seen in the core annihilation data and the experimental results indicate only the magnitude effect. This leads to the conclusion that the Doppler parameters are not affected by the chemical nature of the impurity (Te, Sn, or Si) at the *DX* center.

The reason why the Doppler broadening is not sensitive to the chemical identity of the impurity atom of the DX center is that the trapped positron wave function is rather delocalized. This is also well reflected in the results of Si-doped $Al_xGa_{1-x}As$. The core annihilation parameter decreases in undoped $Al_xGa_{1-x}As$ when the AlAs mole fraction increases.[7] The same happens with the core annihilation parameter of the DX level in Si-doped $Al_xGa_{1-x}As$ when the AlAs mole fraction increases.[7] This means that the wave function of the trapped positron at the DX center strongly overlaps with the second nearest neighbors, i.e., with the Ga and Al atoms.

These arguments show that the positron is very insensitive to the chemical identity of the atoms next to the vacancy in the DX center, and open volume mainly has influence in the S and W parameters. We can thus conclude that the magnitudes of the core annihilation spectra (Fig. 6) give evidence that the open volume of DX(Te) is less than in DX(Si) or in DX(Sn).

The large lattice relaxation model is widely approved to describe the DX center in n-type $Al_xGa_{1-x}As$. In the case of the group-IV(Si) doping, the donor atom itself undergoes a large bond-breaking displacement along its bond axis towards the neighboring interstitial site. It leaves a Ga vacancy behind and as a result a close-pair configuration such as V_{Ga}-Si_i is formed. Recently, positron trapping at this kind of vacancy defect with a small open volume has been observed.[7]

There exist very few theoretical calculations for the vacancy-interstitial model in the case of group-VI(S,Se,Te) doping. It has been estimated that the deep state is formed in Te-doped $Al_xGa_{1-x}As$ when $x>0.26$–0.29.[27] The vacancy-interstitial model predicts that the Te atom sitting on the As site stays fixed, but a neighboring Ga atom is distorted towards the interstitial site and a Ga vacancy is formed in the configuration $DX(\mathrm{Te})=\mathrm{Te}_{As}$-$V_{Ga}$-$\mathrm{Ga}_i$.

The results of this work show that a vacancy is a part of the atomic structure of both DX(Si) and DX(Te) centers. The positron results are thus in perfect agreement with the vacancy-interstitial model for the DX centers related to both group-IV and group-VI dopant atoms. In addition, the positron data give evidence that the vacancy formed in the vacancy-interstitial configuration has smaller open volume in the case of the DX(Te) center than in the DX(Si) center. This observation suggests that the distortion of the Ga atom in the DX(Te) center is slightly smaller than the corresponding relaxation of the Si atom in the DX(Si) center.

V. CONCLUSIONS

In summary, we have studied the local structure of the DX center in Te-doped $Al_xGa_{1-x}As$ by Hall and positron annihilation experiments. In Te-doped $Al_{0.27}Ga_{0.73}As$ we observe a vacancy defect which is correlated with the Te doping and Al alloying. The vacancy can be persistently removed by illumination at 20 K. The measured optical ionization cross section for this transition is $\sigma_0 \approx 4\times10^{-17}$ cm^2. The thermal and optical properties of the observed vacancy are completely similar to those of the DX(Te) center. We associate the vacancy with the atomic structure of the DX(Te) center. The measured results are in perfect agreement with the vacancy-interstitial model for the microscopic structure of the DX(Te) center in $Al_xGa_{1-x}As$. The change $W_v/W_B=0.92$ of the core annihilation parameter is found to be smaller for the DX(Te) center than for the DX(Si) or DX(Sn) center in $Al_xGa_{1-x}As$, indicating that the open volume of the DX(Te) is smaller than that of DX(Si) or DX(Sn).

ACKNOWLEDGMENTS

We acknowledge Professor J.-C. Portal's group at the SNCI-Grenoble and Professor A. Selmi's group at the University of Monastir for collaboration concerning the Hall data used in this work.

[1] G. M. Martin and S. Makram-Ebeid, in *Deep Centers in Semiconductors*, edited by S. T. Pantelides (Gordon and Breach, New York, 1986).

[2] D. V. Lang and R. A. Logan, Phys. Rev. Lett. **39**, 635 (1977).

[3] D. V. Lang, R. A. Logan, and M. Jaros, Phys. Rev. B **19**, 1015 (1979).

[4] P. M. Mooney, J. Appl. Phys. Rev. **67**, R1 (1990).

[5] D. J. Chadi and K. J. Chang, Phys. Rev. B **39**, 10 063 (1989).

[6] L. Dobaczewski, P. Kaczor, M. Missous, A. R. Peaker, and Z. R. Zytkiewicz, Phys. Rev. Lett. **68**, 2508 (1992).

[7] J. Mäkinen, T. Laine, K. Saarinen, P. Hautojärvi, C. Corbel, V. M. Airaksinen, and P. Gibart, Phys. Rev. Lett. **71**, 3154 (1993).

[8] R. Krause-Rehberg, Th. Drost, A. Polity, G. Roos, G. Pensl, D. Volm, B. K. Meyer, G. Bischopink, and K. W. Benz, Phys. Rev. B **48**, 11 723 (1993).

[9] J. Lahtinen, A. Vehanen, H. Huomo, J. Mäkinen, P. A. Huttunen, K. Rytsölä, M. Bentson, and P. Hautojärvi, Nucl. Instrum. Methods **17**, 73 (1986).

[10] S. Mantl and W. Triftshäuser, Phys. Rev. B **17**, 1645 (1978).

[11] K. Saarinen, P. Hautojärvi, J. Keinonen, E. Rauhala, J. Räsänen, and C. Corbel, Phys. Rev. B **43**, 4249 (1991).

[12] M. Alatalo, H. Kauppinen, K. Saarinen, M. J. Puska, J. Mäkinen, P. Hautojärvi, and R. M. Nieminen, Phys. Rev. B **51**, 4176 (1995).

[13] R. J. Nelson, Appl. Phys. Lett. **31**, 351 (1977).

[14] J. Mäkinen, T. Laine, K. Saarinen, P. Hautojärvi, C. Corbel, V. M. Airaksinen, and J. Nagle, Phys. Rev. B **52**, 4870 (1995).

[15] M. J. Puska (private communication).

[16] *Positrons in Solids*, edited by P. Hautojärvi, Topics in Current Physics Vol. 12 (Springer-Verlag, Heidelberg, 1979); *Positron Solid State Physics*, edited by W. Brand and A. Duspasquier (North-Holland, Amsterdam, 1983).

[17] J. Mäkinen, C. Corbel, P. Hautojärvi, P. Moser, and F. Pierre, Phys. Rev. B **39**, 10 162 (1989).

[18] P. M. Mooney, G. A. Northrop, T. N. Morgan, and H. G. Grimmeiss, Phys. Rev. B **37**, 8298 (1988).

[19] G. A. Northrop and P. M. Mooney, J. Electron. Mater. **20**, 13 (1991).

[20] S. Kuisma, K. Saarinen, P. Hautojärvi, C. Corbel, and C. LeBerre, Phys. Rev. B (to be published).

[21] K. Saarinen, P. Hautojärvi, P. Lanki, and C. Corbel, Phys. Rev. B **44**, 10 585 (1991).

[22] C. Corbel, F. Pierre, K. Saarinen, P. Hautojärvi, and P. Moser, Phys. Rev. B **45**, 3386 (1992).

[23] J. Mäkinen, P. Hautojärvi, and C. Corbel, J. Phys. Condens. Matter **3**, 7217 (1991).

[24] R. Krause, A. Klimakow, F. M. Kiesling, A. Polity, P. Gille, and M. Schenk, J. Cryst. Growth **101**, 512 (1990).

[25] M. J. Puska, C. Corbel, and R. M. Nieminen, Phys. Rev. B **41**, 9980 (1990).

[26] M. Alatalo, B. Barbiellini, M. Hakala, H. Kauppinen, T. Korhonen, M. J. Puska, K. Saarinen, P. Hautojärvi, and R. M. Nieminen (unpublished).

[27] D. J. Chadi, Phys. Rev. B **46**, 6777 (1992).